Technical University of Denmark

DTU

McStas

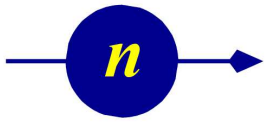

CAMEA

Simulations & Kinematic Calculations

Author:

J. O. Birk

ESS

PAUL SCHERRER INSTITUT

PSI

EPFL

ÉCOLE POLYTECHNIQUE
FÉDÉRALE DE LAUSANNE

Contents

1 Introduction

During the design of CAMEA extensive simulations and cinematic calculations were performed to explore the vast parameter space. These have led to a far better understanding of the instrument performance as well as new ideas to improve the instrument.
Many simulations of the backend were done using a simpler triple axis model of the instrument whereas some frontend simulations and calculations were done a version with a 3 % longer guide (and thus 3 % shorter wavelength band), than what is proposed.

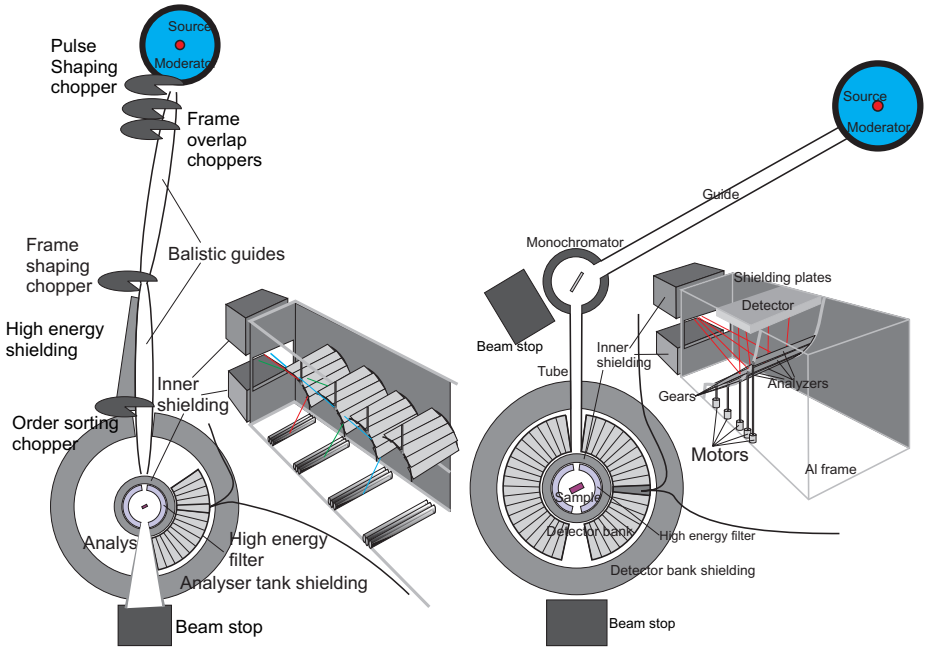

Figure 1: ***Scematic drawings of CAMEA*** *at ESS (left) and a reactor source (right).*

2 Working model

During the simulations and calculations a working model has been used. The model turned out to be so successful that most of it was reused as the final proposed instrument. Because of this almost all results can be transferred directly to the final proposed instrument, and simulations in different sections should be compatible. The newest working model have the following specifications:

- Analyser mosaicity: 60 arch minutes
- Detectors: 3 parallel H_3 tube with a 1/2 inch diameter per analyser *But in a few simulations 7 were used to understand the boundaries better.*
- Analysers crystals: 1 mm deep and 1 cm wide.
- Vertical covering angle: $\pm 2\,\mathrm{deg}$
- Sample size: 0.5*0.5*0.5 cm^3 to 1*1*1 cm^3

Energies of analysers (meV)	2.5	2.8	3.1	3.5	4	4.5	5	5.5	6.5	8
Sample analyser distance (m)	1.00	1.06	1.13	1.20	1.28	1.37	1.46	1.56	1.67	1.79
Analyser detector distance (m)	0.8	0.9	1.0	1.1	1.15	1.25	1.35	1.4	1.45	1.5

3 Coverage

Kinematic calculations were performed to investigate the coverage of the instrument under certain settings, using $\boldsymbol{q} = \boldsymbol{k}_i - \boldsymbol{k}_{\boldsymbol{f}}$ and $k\omega = \frac{\hbar^2}{2m}$ where ToF provides continous coverage of k_i for any k_f.

3.1 Scanning $\mathbf{k}_f$

Figure 2 shows examples of such coverages. It is shown that the optimal scan mode would often be a mode where the analysers were rotated and detectors moved to investigate different E_f values. Some of the displayed effect was found to be replaceable by the idea of getting several energies from one analyser. This together with a continuous sample rotation where data is recorded in event mode will make the performance gain from the E_f scanning mode far too small to justify the extra complexity and cost of such a solution.

To se how this coverage would map out an actual dispersion a magnon were simulated. This was done in the high flux mode where the full pulse length is used and the signal from all 3 detectors looking at a single analyser is integrated. The corresponding 4% energy resolution is the coarsest achievable at the instrument

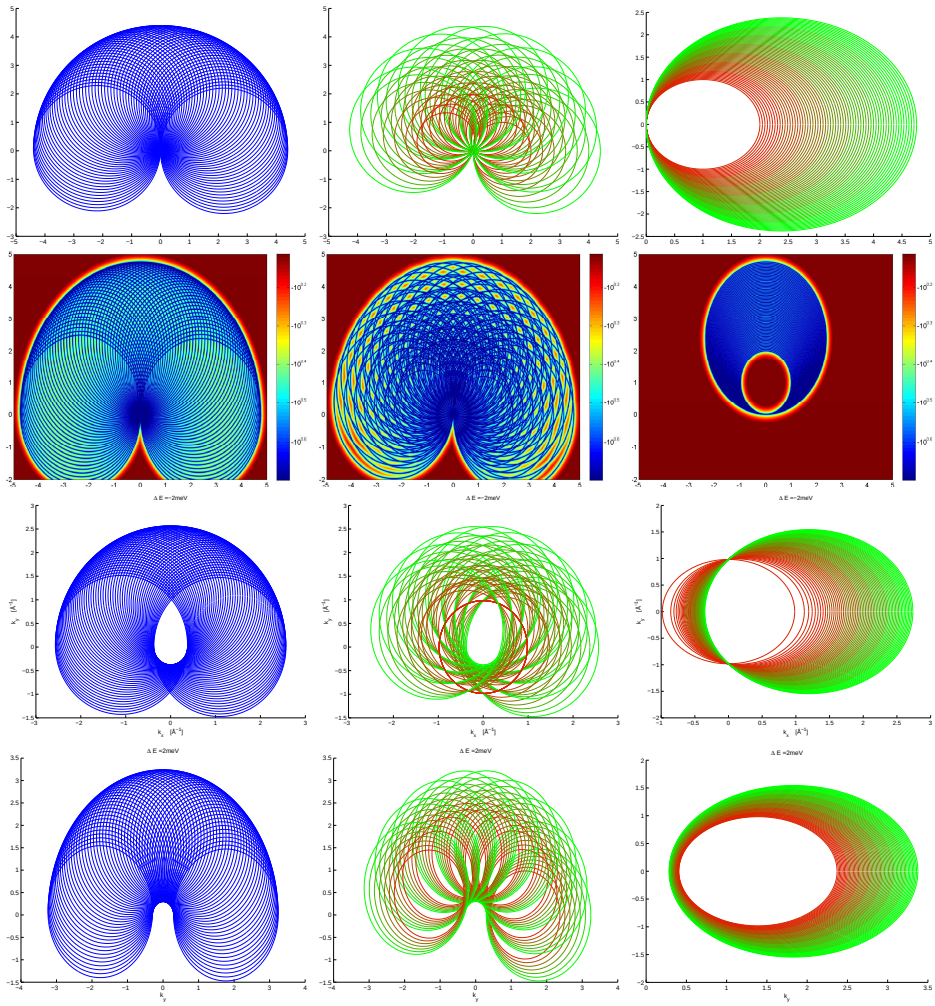

Figure 2: ***Coverage illustrations*** *The figures shows idealised coverage of an ESS CAMEA module at different energy transfers ($\hbar\omega$). First row illustrates the signal at $\hbar\omega = 0$. Left shows a flat-cone-like instrument performing a sample rotation scan in 70 steps while the middle shows the same scan performed by a CAMEA system with 7 analysers but only in 10 steps. Finally the same 7 analysers scan E_f and keeps the sample still. As it can be seen the homogeneity is best for the E_f scan and worst for the CAMEA A3 scan. To further investigate this, a calculation of the distance to the closest measured point was done for all 3 setups. The results are displayed in the second row, again confirming that E_f scans are preferable. Finally the two bottom lines shows the inelastic coverage at Δ E = -2 meV and Δ E = -2 meV. The calculations were done before the work model were established with a different distribution of E_f values but the principle will also be true for the work model.*

meaning that the count rate in each pixel will be comparable to that of a triple axis instrument with doubly focusing monochromator and focusing analyser. All energies and angles correspond to those of the work model. The energy band

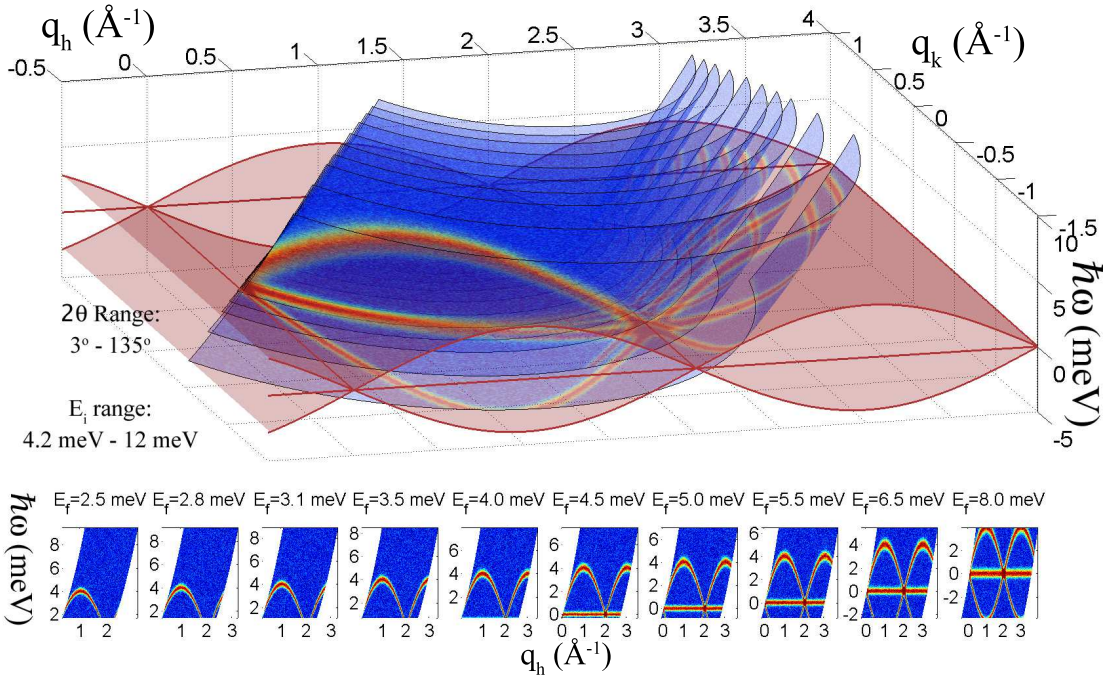

Figure 3: Simulated coverage of magnon dispersion. The signal corresponds to a single data accusation without dark angles and in high flux/low resolution mode.

has been decreased slightly when the pulse shaping chopper was moved to 6.5 m after this work was done.

3.2 Dark Angles

The CAMEA design has a quasi-continuous angular coverage of the horizontal scattering plane with gaps in the two theta coverage. The main contribution to these gaps comes from the flat analysers reflecting out of the plane, but even if curved analysers were chosen gaps for walls, analyser mountings and collimators would produce small dark angles. In order to cover these gaps the CAMEA analyser-detector module will be designed to be able to rotate a few degrees thus covering all two theta angles in its range by measuring two different settings or 2 times in 3 settings. There are however also possible to cover the plane by simply rotating the sample (a3) slowly around. This method will lead to a non-uniform statistical and resolution coverage but will still be useful for many experiments. Note that this work has been compiled before any technical drawings have been made. It is quite possible that we will get bigger or differently distributed dark angles in the final design but these will not change the principles described here.

3.2.1 Discrete rotation of a3

In many cases scans will be done with a series of discrete a3 steps. If that is the case the coverage will look as in figure 4. The covered area is without gaps, but

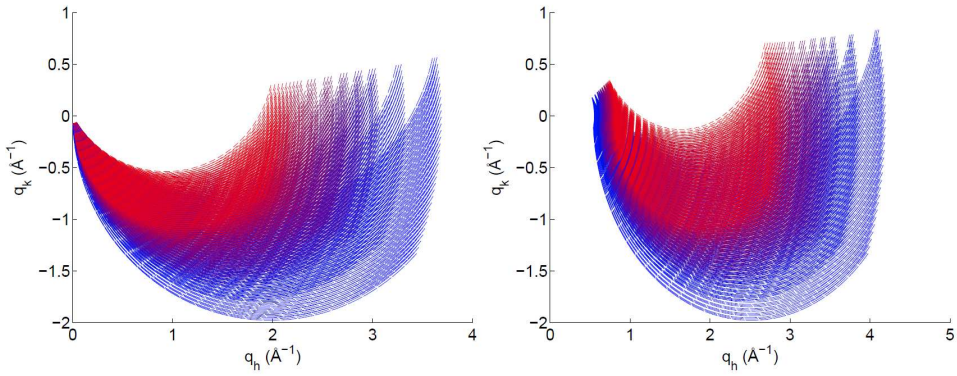

Figure 4: Examples of how the reciprocal space would be covered by a discrete sample rotation. Left: 0 meV energy transfer. Right 5 meV energy transfer. Each line represents the centre of the measurement from one specific analyser. The red lines are low E_f (fine resolution) and the blue high E_f (coarse resolution). The sample is rotated 30° in discrete steps of 1°.

some areas have gaps in the fine resolution data fine resolution data (red lines in the figure). It is however hard from the figure to quantify the gaps. Hence we will continue to the case of continuous a3 scanning in section 3.2.2 as it makes it the coverage clearer and the results can be generalized to the discrete case. Note that the 1.7 Å wavelength band accepted by CAMEA does not allow all analysers to display the elastic line at the same time, unless every second moderator pulse is removed by the chopper system. The exact number of analysers that can see the elastic line depends on the choice of wavelength band. On the other hand all analysers can see the 5 meV energy transfer line at the same time if the wavelength band is chosen with this in mind.

3.2.2 Contious rotation of a3

With the high flux and event mode data acquisition of ESS-CAMEA it is foreseen that many experiments will be done rotating the sample slowly around while counting. This will lead to a coverage as shown in figure 5. The gaps in the coverage from the first analysers are now clearly visible but it is also clear that all gaps are covered by analysers behind the front most ones. Only the small gaps in the regions exclusively covered by the backmost analyser are left open. It can be seen that the analyser overlap changes with both the scattering angle and energy transfer so it is impossible to design the dark angles and energies in a way so no gaps will be seen between the first two analysers for all energy transfers. This means that some areas will have lower statistical weight and a coarser resolution than others when the dark angles are only covered by a3 rotation. Note that the 7th analyser is at 5 meV - the most used energy for cold triple axis spectroscopy. Hence if just one of the first 7 analysers covers the region, then the resolution will be better than in many cold triple axis experiments. In addition the distance collimation means that CAMEA has a q-resolution a well collimated triple axis

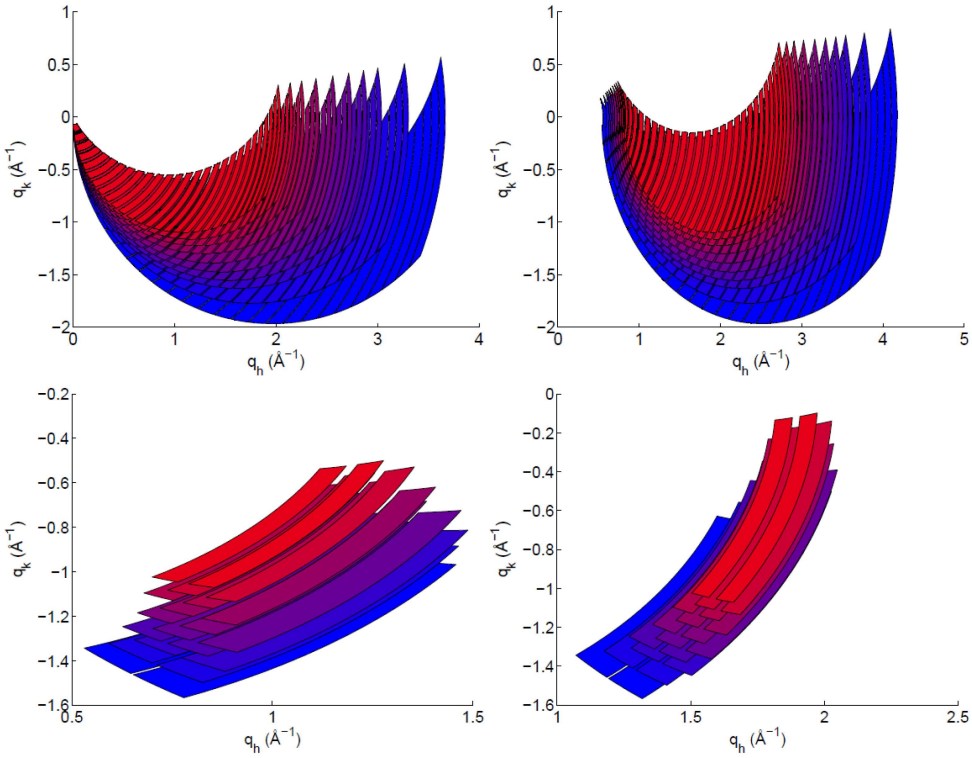

Figure 5: Examples of how the reciprocal space would be covered by a continuous sample rotation. Left: 0 meV energy transfer. Right 5 meV energy transfer. Each coloured area represents the area covered by one analyser when the sample is rotated continuously through 30 degrees. The red lines are low E_f (fine resolution) and the blue high E_f (coarse resolution). The top row shows all analyser segments whereas the bottom row only shows two. As the coverage changes with energy the same segments are not displayed for all E_f values but instead segments covering approximately the same area in reciprocal space are chosen.

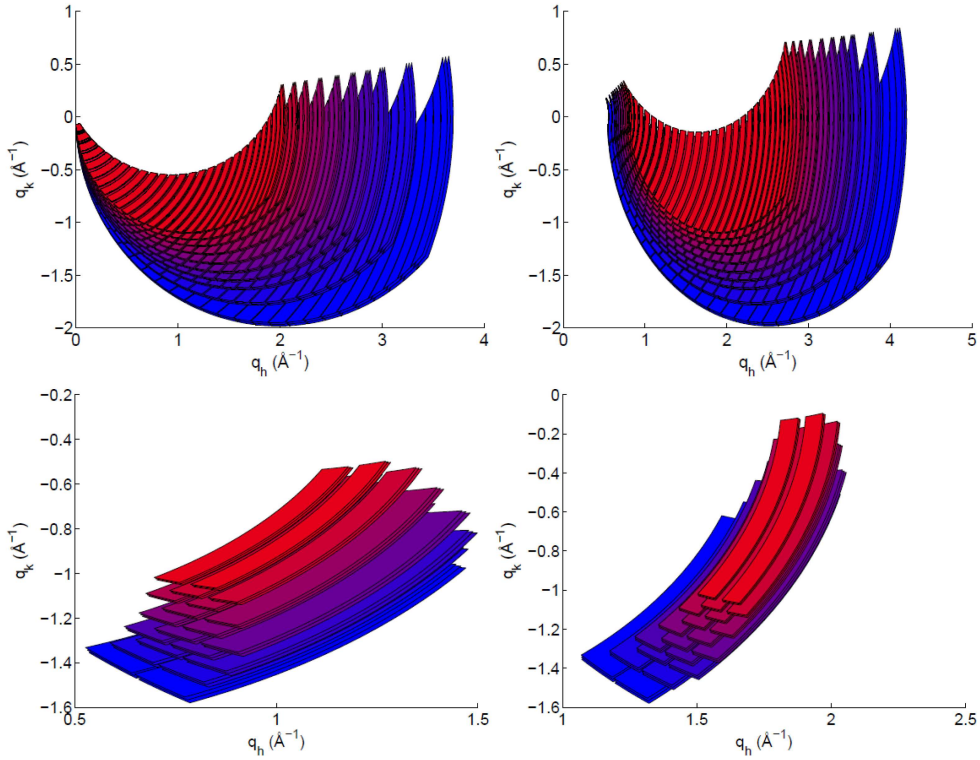

Figure 6: Examples of how the reciprocal space would be covered by a continuous sample rotation with 3 energies from one analyser. The same as in figure 5 but with 3 half-inch tube detectors 0.5 mm apart looking at the same analyser.

instrument and better Energy resolution.

3.2.3 Multiple energies from one analyser

As described in detail in section 7.2 it is planned to obtain 3 different energies from each analyser. If this is taken into account the gaps between the analysers becomes even smaller, though they are still there for the front most analysers (se figure 6). If one chose to collect 5 energies from each analyser the gaps would generally de covered (se figure 7) but there would still be a big difference in statistics. Partly because some areas are only covered by one energy per analyser and partly because the outermost energies from each analyser will have lowers statistics due to the mosaicity of the analysers. The later can be reduced by choosing analysers with a more relaxed mosaicity but the former will still be true.

3.2.4 Usefullnes of the a3 scan mode.

Although the a3 scan mode does have its limitations in covering the dark regions of the scattering angles it will be useful for many experiments. If one needs the a3 scan anyway which most mapping experiments will then CAMEA will make

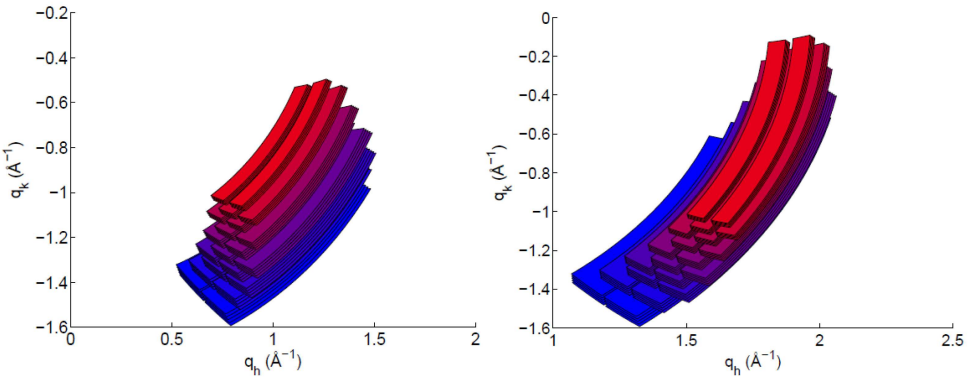

Figure 7: Examples of how the reciprocal space would be covered by a continuous sample rotation with 5 energies from one analyser. The same as in figure 5 bottom but with 5 half-inc tube detectors 0.5 mm apart looking at the same analyser.

a continuous coverage of the chosen part of reciprocal space, without rotation of the analyser tank. Not all areas will have the sample resolution or the same statistics but it should be possible to cover all areas with a resolution better than what is seen on typical triple axis experiments and statistics from at least half the analysers. Should the generated map show features in the regions where the resolution are limited the user can afterwards rotate the analyser-detector module and redo the scan.

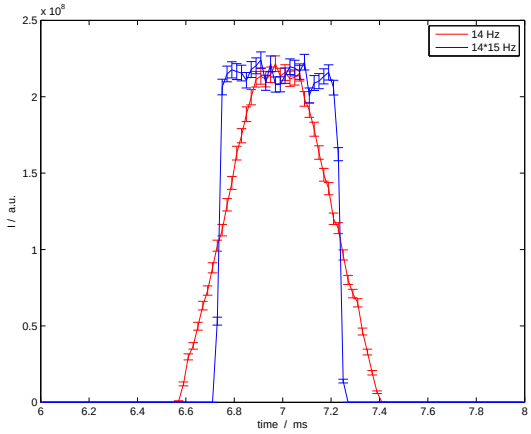

Figure 8: The pulse just after a pulse shaping chopper running at 14 Hz and 210 with 0.5 ms opening at a 1 cm pinhole. While the intensity is roughly the same the 210 Hz chopper has a much shorter opening/closing time.

4 The Chopper system

The instrument will ideally need 7 choppers, located at 6.5, 6.5, 8, 13, 78, 162, and 162 m. The reason for the choppers and their positions will be explained below.

4.1 Pulse shaping choppers

A pair of disc choppers placed 6.3 - 6.5 m from the moderator with a radius of 35 cm, an opening of 170°, and a variable frequency of up to 300 Hz
A pair of disc shoppers should be placed as close to the source as possible to shape the pulse from the moderator (denoted "the main pulse"). The geometrical restrictions close to moderator are rather strong if not 100 % well defined, so we are limited to 35 cm disc choppers at maybe 6.5 m from the moderator.
These pulse shaping choppers define our instrument resolution so it is important that they open and close as fast as possible to minimize the energy tails. The geometrical restrictions make it impossible to achieve this with bigger choppers so we have to change the opening and closing in other ways:
We can design the guide with a needlepoint at the chopper position. This will help us get a better opening time but significant tails can still be observed at high resolution settings for 14 Hz frequency (se figure 8).
We can spin the pulse chapping choppers faster at $n_{pulse} * 14$ Hz and make the opening n_{pulse} times bigger also making the opening and closing n_{pulse} times faster. Exactly how fast we can run the choppers depends on the desired pulse width but for 2 ms the limit is $n_{pulse} = 15$ which is sufficient to give a well-defined pulse also for all relevant opening times. ESS has no problems with choppers so close to the moderator running at high frequencies as long as they are otherwise standard choppers.

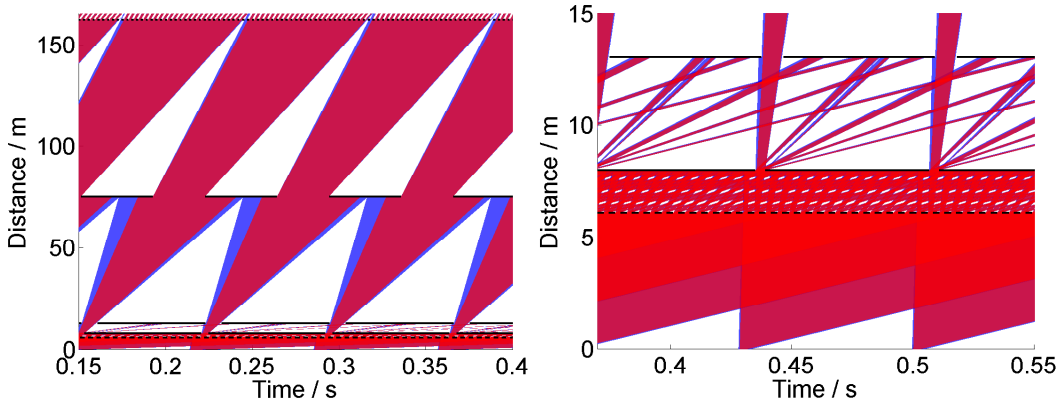

Figure 9: Left: Time of flight diagram for the proposed chopper system. The order sorting chopper system is not included for simplicity. Right: Details of the first 20 m's of the chopper system.

4.2 Frame overlap choppers

Two disc choppers placed 8 and 13 m from the moderator with a radius of 35 cm, frequency of 14 Hz, and an opening of ∼20° and ∼45°
In order to remove $n_{pulse} - 1$ of the sup pulses from each main pulse and remove crosstalk between two different main pulses two extra choppers are needed: One as close to the pulse shaping choppers as possible to remove the sup pulses and one further away where second order pulses can be separated from first order pulses. The exact positioning can be modified but could for example be at 8 and 13 m, where 8 is chosen relatively close to the pulse shaping system and 13 far enough away to be outside the inner biological shielding for simpler maintenance.

4.3 Tail removal chopper

A single disc chopper placed 78 m from the moderator with a radius of 35 cm, an opening of 157.6°, and a frequency of 14 Hz
Though the tails of the moderator are removed from the resolution function by the pulse shaping choppers the tails do still have an effect on the width of the entire pulse at the sample position. It will severely limit the useful bandwidth if these tails are not removed. The chopper doing this should be as close to the sample as possible in order to remove as much tail as possible but far enough away that two neighbouring pulses can be separated. The limit turns out to be close to 78 m where our guide design is narrow due to the bending section.

4.4 Order sorting chopper

Two disc choppers placed 3 m before the sample of radius 35 cm, two openings of ∼ 80°, and a frequency of ∼ 180 Hz
To distinguish first, second, (and possibly third) order scattering from the analysers a pair of choppers are installed as close to the sample as possible. The

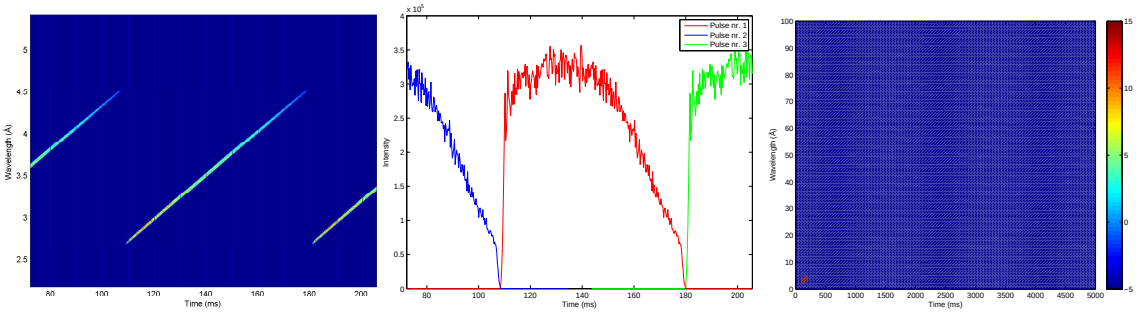

Figure 10: Left: McStas simulation of the pulse shape in a (t,λ) diagram. Middle: Collapsing the data to the time axis it is clear that two neighbouring pulses can be distinguished well. Right: Zoom out on log scale showing that no long wavelength neutrons (up to 100 Å) makes it through to the sample. Note that McStas as default only generates one pulse so in the first two figures this pulse have been repeated in Matlab with a frequency of 14 Hz while the last only show this single pulse. All simulations are done at 2ms chopper opening 14*15Hz pulse shaping chopper speed and a lowest transmitted energy of 4 meV (4.5 Å)

choppers will be running at close to 360 Hz slightly depending on the final geometry and while this is not a problem for normal choppers it is a question how well this will work close to a 25 T magnet. If we only want to distinguish first and second order scattering, while assuming higher orders to be insignificant, a single chopper is enough but if we want more freedom to also separate higher orders two choppers will be needed.

4.5 Other possible choppers

A t_0 chopper could be useful to remove the prompt pulse but may not be needed as we bend the guide out of line of sight.

4.6 Solutions with fewer choppers

It is possible to reduce the number of choppers but not without reducing the efficiency of the instrument significantly. Most obvious solutions would be to keep the pulse shaping choppers at 14 Hz and go for a single order sorting chopper, accepting the less desirable pulse shape, and removing the order sorting choppers to go for a filter solution instead.

4.7 Performance of Chopper system

The chopper system has been simulated and shown to block all unwanted neutrons in the range from 0.1 to 150 Å for a range of different wavelength bands, opening times and pulse shaping chopper speeds. An example of such a test can be seen in figure 10. Simulations of the energy resolution (see figure 11 shows that it is possible to vary it from 3% at 5 meV down to 0.3%. This makes it possible to tune it to give resolution matching anywhere in the entire dynamic

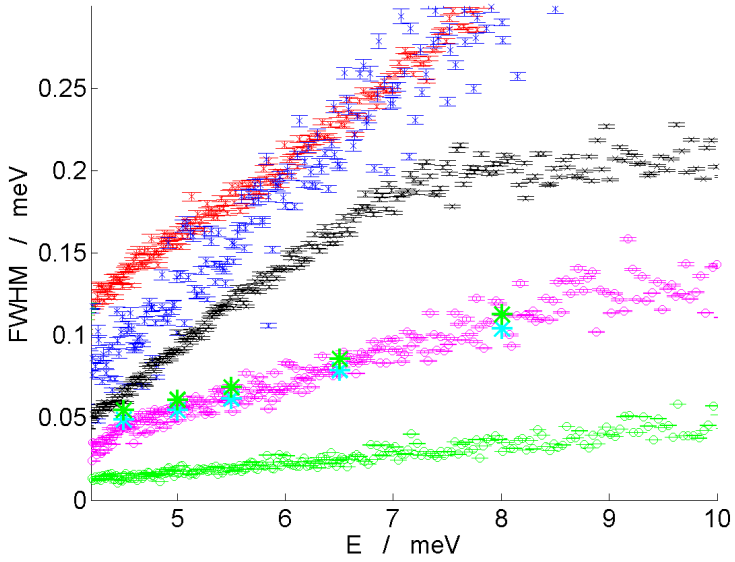

Figure 11: Energy resolution of the chopper system for varying opening times of the pulse shaping choppers. Red: full open, Blue: 5 ms, Black: 2.9 ms, Magenta: 1 ms, Green: 0.1 ms. The blue and green single asterisks are analytical and simulated resolutions of the secondary spectrometer for comparison.

range of the instrument and to unmatch the resolutions to push either flux or resolution above the standard operating numbers. The high possible resolution also enables precision measurements of powder lines e.g. needed to determine the pressure for high pressure experiments.

4.8 Order sorting

By placing a chopper a few meters before the sample it is possible to distinguish first and second order scattering on the analysers from the flight time. In principle one can have a chopper opening time of 50% but with flight time uncertainties, chopper opening and closing times and the fact that placing all detectors from the different analysers at the same optimized distance means that opening times of about 40 % is more likely. Of cause this leads to a flux on sample reduction of 60 % but at the same time the coverage is doubled and the Be filter removed together with its beam attenuation so the number of neutrons counted on the detector will not suffer as much.

The system would perform best with the choppers running at 360 Hz just before the sample but as a chopper with a single opening of $\sim 50\%$ is unbalanced and hard to run at these frequencies and it is foreseen to mount 25 T magnet on the instrument leading to strong stray fields the performance at different number of openings and distances to the sample was done (se figure 13). Based on the results two openings and 180 Hz was chosen as it makes the chopper far more stable and it was moved back to 3 m from the sample. Here the stray field

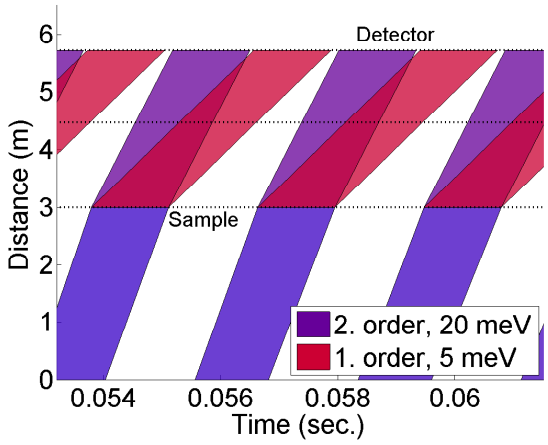

Figure 12: ***Order sorting for one analyser.*** *The graph only shows a limited part of the wavelength band as it would otherwise become extremely messy.*

is expected to be 300 times lower than the limit given by chopper producers making the chopper more reliable.

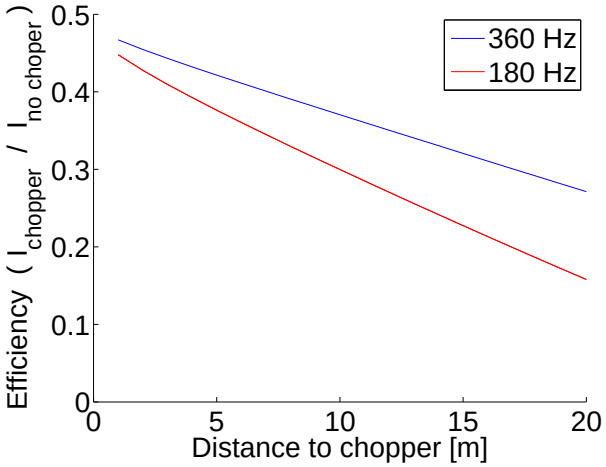

Figure 13: ***Performance of order sorting chopper.*** *The 180 Hz chopper has two symmetric openings while the 360 Hz chopper has a single large opening.*

4.8.1 Higher orders

It is in principle possible to use choppers to distinguish higher orders by closing the order sorting choppers more but the loss factor will be higher.

4.9 Chopper phase uncertainties

The long pulse of ESS and corresponding long primary flight path makes the instrument more resilient to phase uncertainties than many other instruments.

Since the radius of the choppers are not scaled together with the timeframes and instrument lengths one can either relax the frequency or produce choppers with bigger openings. The choppers most sensitive to phase uncertainties are for CAMEA chosen with very big openings, and that reduces the phase uncertainty problem significantly. Below is a description of how phase uncertainties in each chopper will influence the performance of the chopper system.

4.9.1 Pulse shaping choppers

Phase uncertainties in the pulse shaping choppers can in principle both lead to a lower intensity and a wrong determination of λ_i. Both effects will be very small due to the big opening of the choppers. A phase uncertainty of 1° leads to a drop in flux of less than one percent and a wrong determination of λ_i of the order 0.01%.

4.9.2 Frame overlap choppers

The frame overlap choppers are independent of phase uncertainties up to about 5 degrees, since they are not shaping the actual beam but only removing unwanted pulses.

4.9.3 Frame shaping chopper

The frame shaping chopper will shift the wavelength band if out of phase. The shift can however be determined and will not influence the resolution and intensity at a given wavelength. A shift of 1∘ on the chopper and will lead to a shift of the wavelength band of about 0.5 % of the lowest selected wavelength. In principle the width of the wavelength band can be reduced but for the proposed chopper system this will only happen if the chopper is more than 10° out of phase and can thus be ignored.

4.9.4 Order sorting chopper

Phase shift in the order sorting choppers will shift each pulse and can in principle lead so a loss of flux of 1.5% for 1∘ if the phase shift is unknown but since phase shifts can be determined by both direct measurements and data analysis the effect becomes negligible.

5 Analysers

5.1 Analyser Materials

Different materials were considered for analysers. Pyrolytic Graphite is commonly used for cold monochromators/analysers and has several nice characteristics:

- The peak reflectivity is very high.

Material	Attenuation though 1 blade at 45° (%)	Reflectivity (%)	Thickness (mm)
PG	0.01	75	1.0
Si	5.34	40	20.0
Ge	17.5	40	6.0

Table 1: ***Analyser materials.*** *Attenuation calculated from data from [1] at 0K. At room temperature 2mm PG has been measured to have an attenuation of 2% a 5 meV. Above this energy, the attenuation increases strongly.*

- The attenuation is low, even more so when considering the low thickness needed.
- No other Bragg peaks will be an serious issue even with a relatively open geometry.

It does however also show a number of drawbacks:

- Crystals are relatively small so a wafer material is needed.
- PG is expensive, especially considering the huge analyser area needed.
- Phonon scattering is a real issue and leads to Lorenzian energy tails. It is thus not ideal for quasi elastic and near elastic studies.

As the drawbacks are considerable, other materials was investigated as well. Si, Ge and Cu are all harder and thus decreases the phonon scattering issue. But unfortunately they have a higher attenuation at sufficient thicknesses and coupled with their lower reflectivity would lead to much lower total count rates. The attenuations at 0 K can be seen in table 1. Although the difference is small for room temperature analysers it is clear that PG is superior for transmission geometries.

For the prototype PG mounted on Si wafers are thus used. Since the cost of PG is proportional to its volume we have gone with 1 mm thickness. It displays almost as good reflectivity for cold neutrons as 2mm but comes at half the cost and with lower attenuation. It is mounted on 1 mm of Si (4,0,0) wafer. The orientation means that $k_{Si} = 2.3 * k_{PG}$ so the Si reflection lies at energies $\sim$5 times higher than PG and thus does not even interfere with the second order reflection. Besides the extremely low mosaicity of Si means that the reflection is weak.

5.2 The asymmetric Rowland Geometry

The analysers will be mounted in an monochromatically focusing Rowland geometry. Since constraints in space, dark angles, order sorting chopper geometry and price makes it difficult to have equal sample-analyser and analyser-detector distances we will need to use the asymmetric Rowland geometry for at least some of the analysers. This means that we cannot use bent analysers and there will be

a small difference in flight time from different parts of the analyser (Se 8.1). The first can however be solved satisfyingly by the use of a piecewise curved analyser, whereas the time broadening has a small influence for time resolved studies but can be neglected for the energy resolution because of the long primary flight path.
In the plain it is possible to curve the analysers, but that would be expensive, limit transmission and severely limit the q-resolution. So instead a piecewise linear setup is suggested.

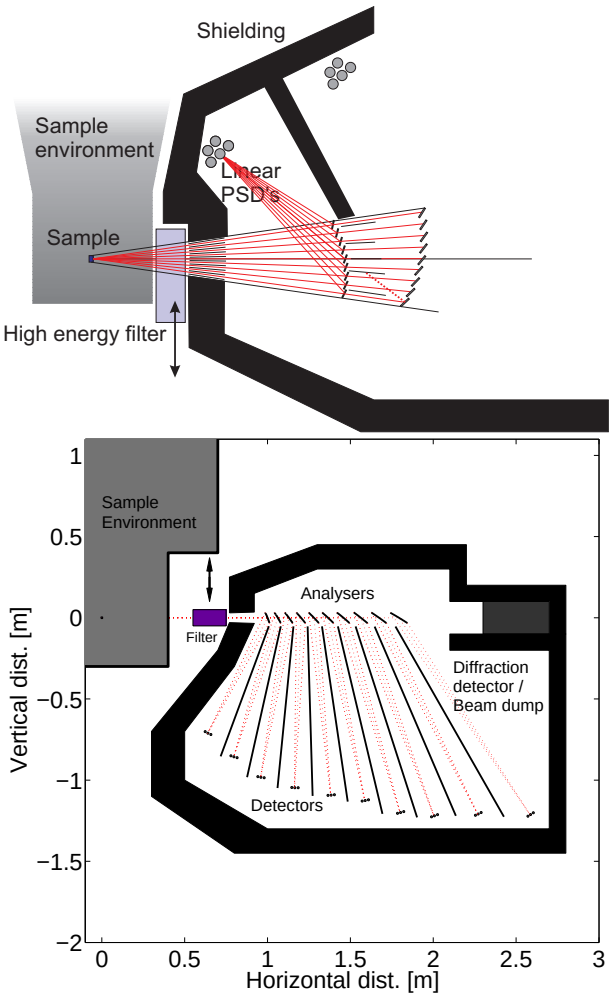

Figure 14: *Top:Illustration of the Asymmetric Rowland Geometry. Bottom: Example of an entire analyser setup with work model numbers.*

5.3 Resolution

The simulated and calculated resolutions can be seen in figure 15. The angular resolution decreases with analyser energy due to the longer distances to the backmost analysers. The angular resolution worsens with higher mosaicity and analyser-detector distances so either one have to limit those, accept a limited q-resolution, or insert collimators. Limiting the mosaicity is expensive and will reduce the flux in the outer detectors, whereas limiting the analyser-detector distance costs energy resolution, time resolution, and increases the phonon tails of the graphite. The chosen numbers will guarantee a good angular resolution while matching different time resolution contributions and giving a very good energy resolution.

The energy resolution can be extremely good in this setup. This is due to the

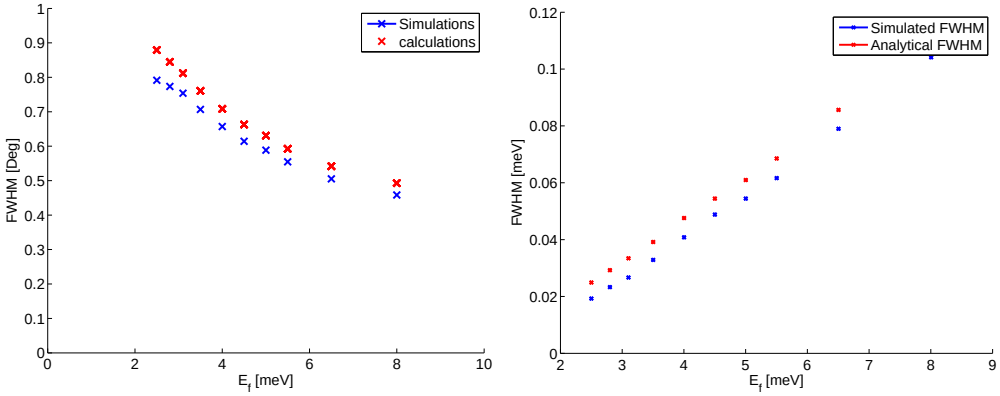

Figure 15: ***Angular and E resolutions.*** *Simulated and theoretical resolutions of the backend. Left: Angular resolution, right: Energy resolution. for all 10 analysers in the work model.*

small sample (1x1 cm), small analyser and detector sizes, and the long distances. Note that one can always worsen resolution by combining data from several detectors. This will indeed often be done as it fits with the incoming resolution of the high flux mode. The good resolution will however still be a key feature of the instrument, and will also be important for time resolved experiments and when the order sorting choppers are running.

Since distance collimation is the main contributor to the energy resolution, and the flight paths to the high energy detectors are longer that to the low energy detectors, the energy resolution changes less with energy than on a normal triple axis instrument. The change is however still more than a factor 5 so it is not possible to combine all data together without advanced data analysis, but the change will be smaller than it would be if a corresponding energy scan were made on a normal triple axis spectrometer.

The q resolution is dependent on E_i, E_f, pulse width, scattering angle, and direction through the ellipsoid. It is not possible to these settings to a single meaning full figure, but the powder resolution at the elastic line for 1 ms opening time of the pulse shaping chopper system can be seen in figure 15

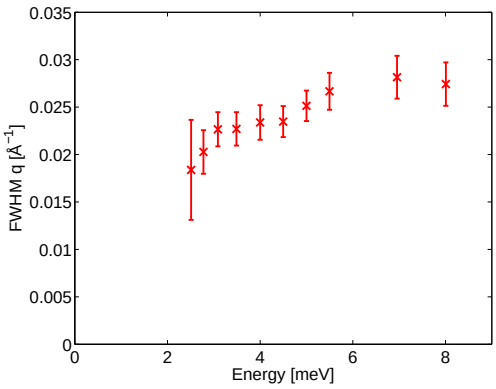

Figure 16: ***q resolution.*** *Simulated q resolution for the full instrument at 1 ms neutron pulse and elastic scattering.*

5.4 Angular coverage of a flat Rowland analyser

Figure 17 describes how the resolution and intensity changes when the analyser is no longer perpendicular to the incoming beam. As it can be seen the geometry works well out till an angular coverage of $\pm 10^\circ$ whereas the final setup only covers $\pm 3^\circ$ for each analyser segment.

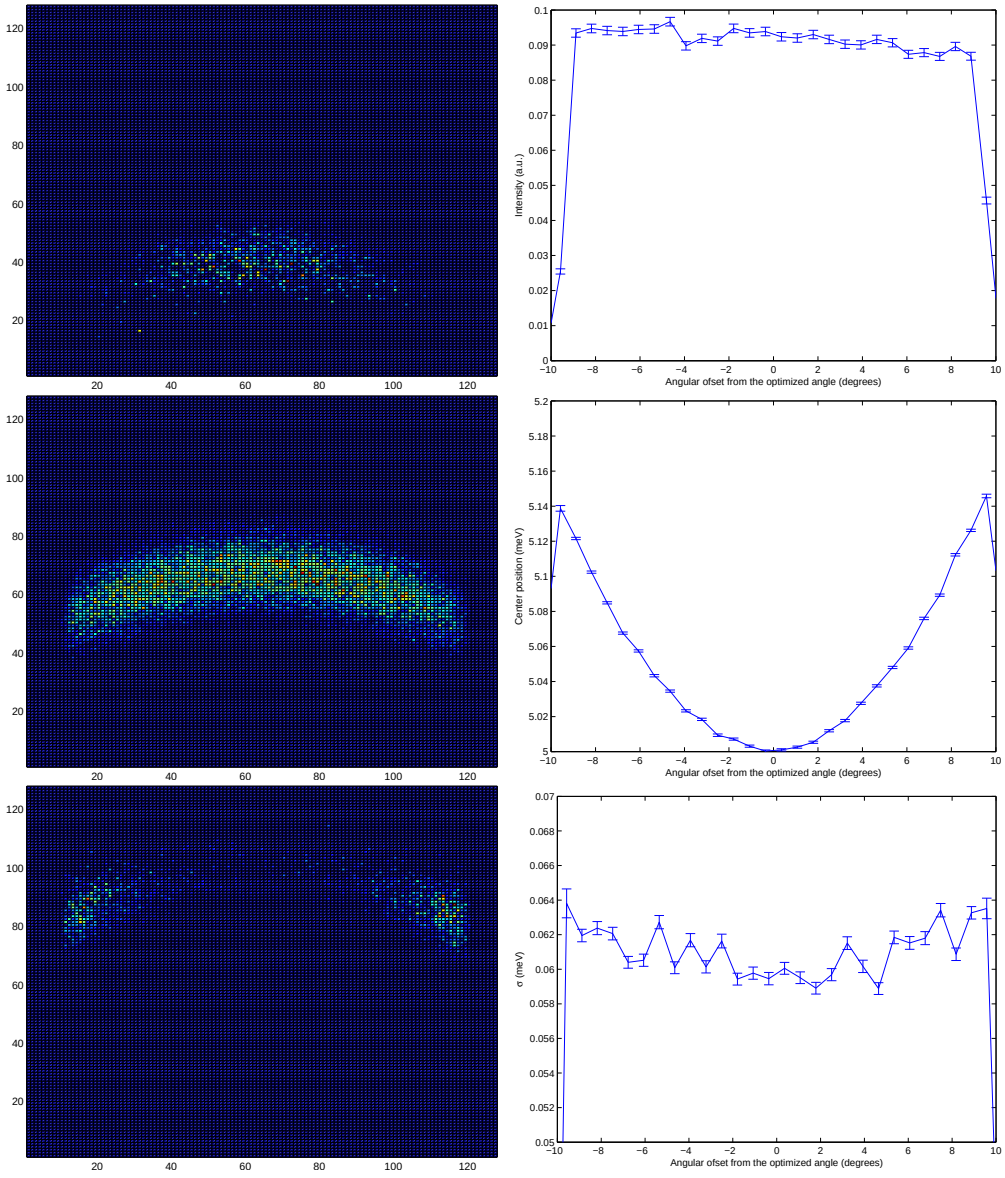

Figure 17: ***Width of detector.*** *Left: PSD view of beam reflected from the analyser for energies below (top), at (middle), and above (bottom) the analyser energy. Right: The Intensity (top), centre point (middle), and width (bottom) a function of angle. The small change in resolution corresponds to the change in measured energy.*

5.5 Rotation of Analysers

The Asymmetric Rowland Geometry was also tested with respect to a θ, 2θ rotation of the analysers and detectors. The result shows that it is indeed possible to scan k_f without a big drop in performance but it was decided that the gain from having this option would not out weight the additional cost and technical complications of such an instrument.

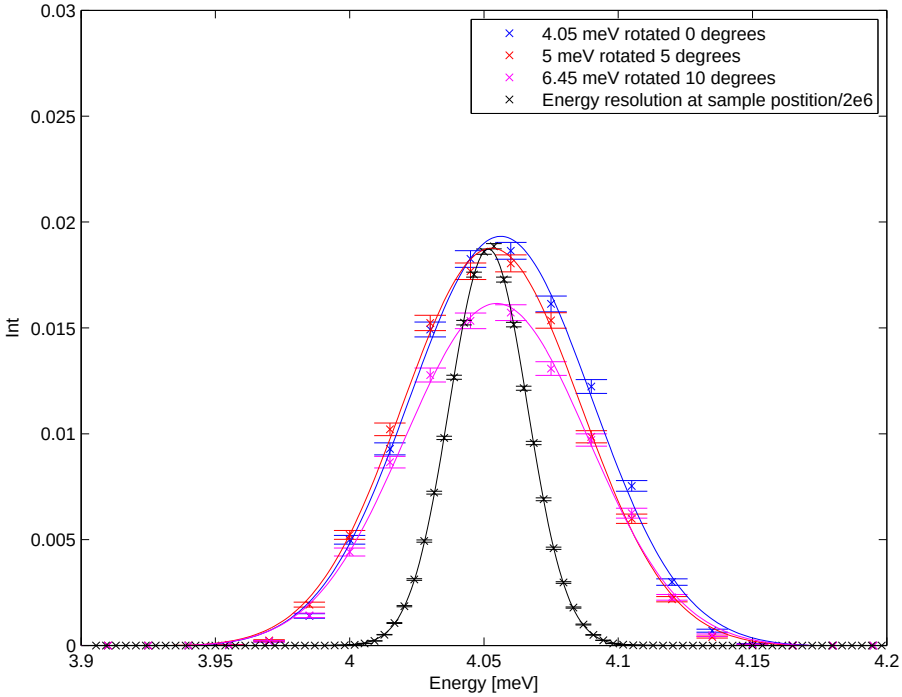

Figure 18: ***Rotating Analysers.*** *A Rowland analyser works fine if rotated 5°. The simulations were done for the full resolution of a triple axis instrument but the (artificially low) incoming resolution (displayed in black) does not dominate the full resolution.*

6 Detectors

All simulations were done assuming He^3 detector tubes, since this is what the prototype has and the technical details of the solid state detectors are still rather uncertain. At the initial simulations a psd was used and the relevant regions were cut out to simulate actual detectors. Later a special detector component was developed for McStas in order to make precise simulations of the instrument performance. This 1d psd with time resolution incorporates time delays and position uncertainty due to the unknown detection depth of the neutron and calculates realistic absorption strengths depending on whether the centre or edges of the detector was hit. The detector has been used for many of the performance studies.

It was also considered if a lower than usual gas pressure would be beneficial in suppressing the thermal background compared to the cold signal. Figure 19 shows how it is possible to dampen the thermal background a factor 2 for 5 meV neutrons using very inefficient detectors. This does however not outweight the loss in detector efficiency and would make the option of recording second order neutrons by using the order sorting inefficient due to the low detection rate at the second order wavelength.

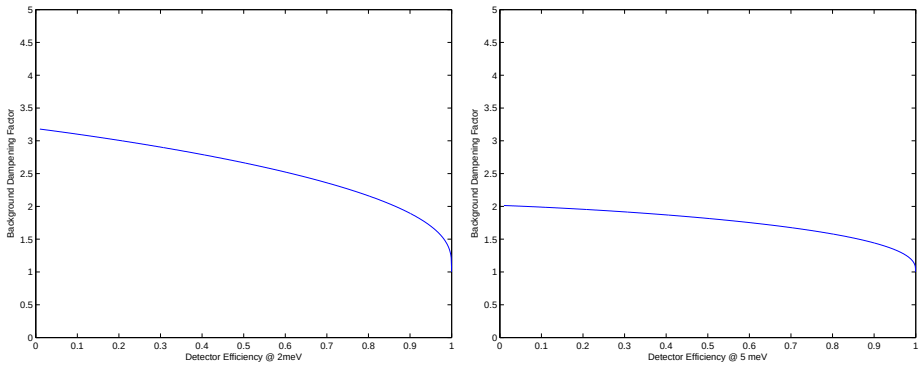

Figure 19: ***He pressure.***

7 Additional issues on Analyzer-Detector interaction

7.1 Mosaicity

The influence of analyser mosaicity on the energy resolution and intensity was simulated. The result can be seen in figure 20. It can be seen that the resolution for a single tube does not depend on the mosaicity. This is because the distance collimation dominates the resolution. For the 3 tubes the distance collimation is less strong and the mosaicity do influence the total resolution.

The intensity does not take the lower peak reflectivity of the graphite into account. In order to investigate this a simple Monte Carlo routine was written to estimate the influence of analyser thickness and mosaicity on the peak reflectivity. The result are shown in figure 21 and shows a limited influence of reducing the mosaicity. The model is very rough but the main findings were later confirmed with prototype data.

Simulations of how the q resolution of the spectrometer depends on the analyser mosaicity can be seen in figure 22. Since the long analysers makes the distance collimation extremely rough in the angular direction the angular resolution does depend on the mosaicity.

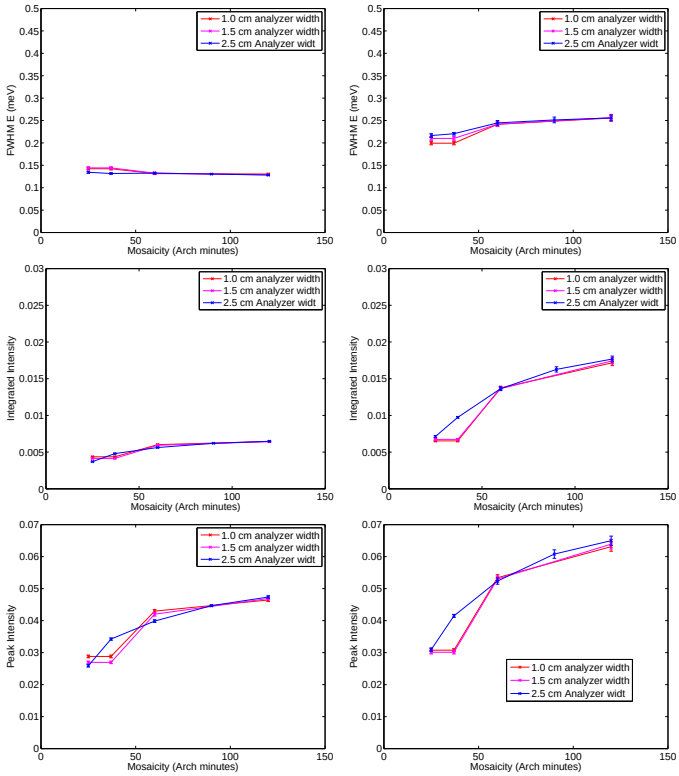

Figure 20: ***E resolution and Intensity for different mosaicities*** *Top: Energy resolution (left), Integrated intensity (middle) and Peak intensity (left) for one* $\frac{1}{2}$ *inc detector tube, Bottom: the same simulations for integrated intensity in 3 three tubes. For one tube higher mosaicity simply gives better resolution and higher intensity. For wider detectors it is a trade-off between resolution and intensity. The work was done with* $E_f = 5$ *meV, 1 cm sample and 1.2 m sample to analyser and analyser to detector distances. Note that a slight decrease in peak reflectivity with higher mosaicity was not included in the model.*

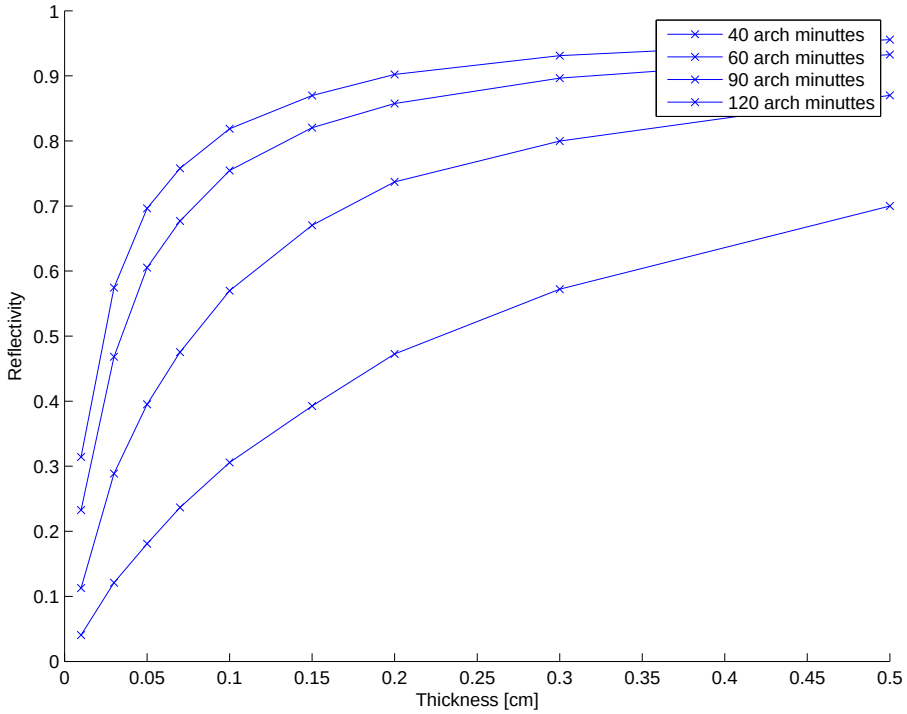

Figure 21: ***Approximate reflectivity of PG as a function of mosaicity & thickness.*** *The reflectivities are found through a simple Monte Carlo model described in 7.1*

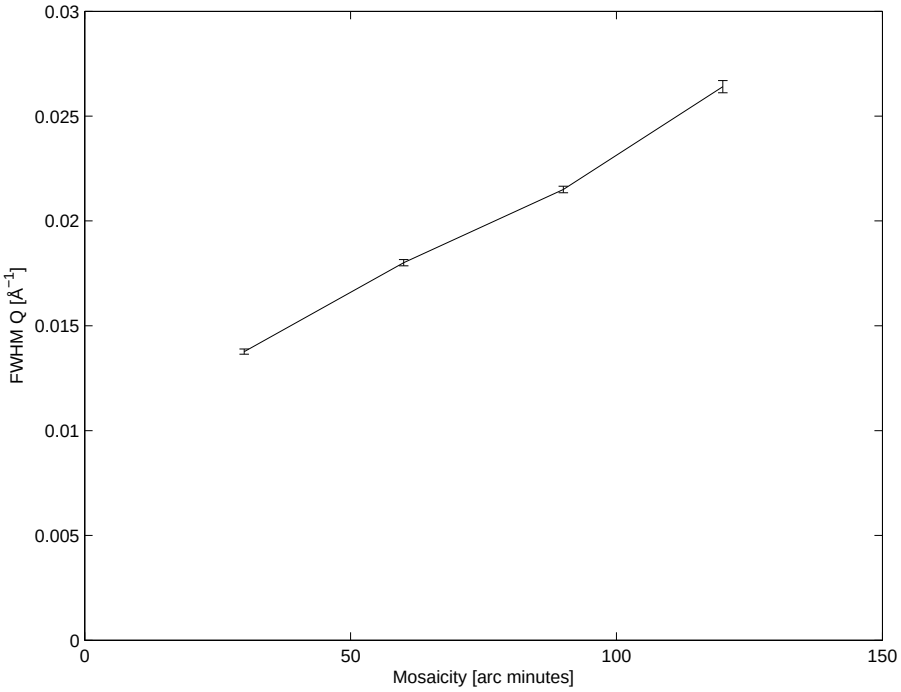

Figure 22: ***Q resolution of CAMEA on a TAS*** *The resolution is a constant contribution from incoming divergence, sample size and detector resolution plus a varying effect from the different divergences. Same settings as in figure 20 was used except for that the energy was 3.5 meV.*

7.2 Several Energies

In our coarse-mosaic analyser set up neutrons with slightly wrong energies are also scattered and will reach the detector surroundings. It is thus possible to detect these in other detectors and thereby increase the total number of counted neutrons without suffering worse energy resolution. This section looks into how well this works in a Rowland geometry and how intensity, resolution and number of detectable energies varies with different mosaicities.

7.2.1 The Principle

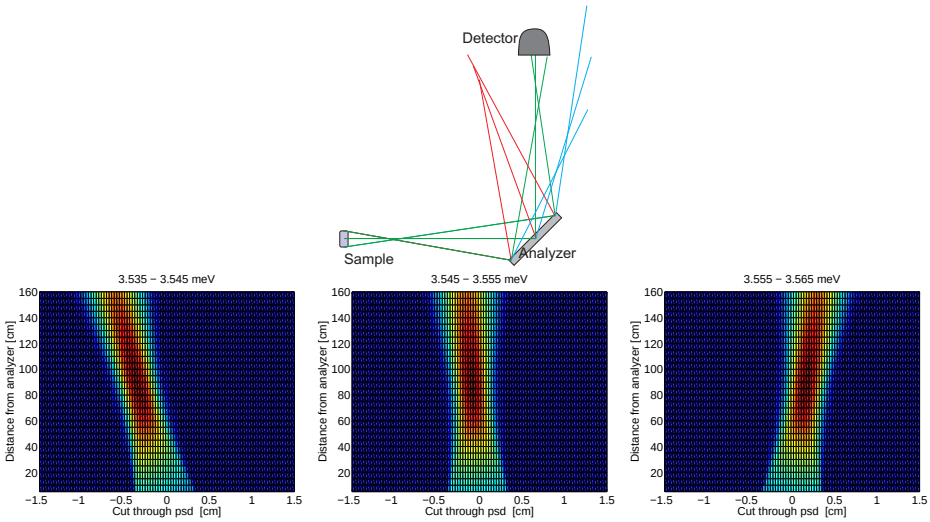

Figure 23: ***Principle of energy selection.*** *Top: Schematics of how an analyser reflects different energies at different angles and focus them at a certain distance. Bottom: McStas simulations the beam profile from a single reflecting analyser for 3 narrow energy bands when the analyser is optimized for the central energy band. The vertical axis is the distance from the analyser and the horizontal axis is transverse to the main beam as in the top panel*

The geometry of a Brag reflection from a flatt analyser slab with a finite width and mosaicity ensures that the desired energy is focused towards one spot whereas other reflected energies is reflected in other directions. (See figure 23). By the right use of distance collimation the energy resolution becomes almost mosaicity independent for relevant mosaicities while the intensities increase with mosaicity before reduced reflectivity and extra q-collimation is taken into account. Another promising use of this effect is to separate different energies reflected from each analyser and thus measure several energies from each analyser.

7.2.2 Simulations

To investigate this effect by simulations a Rowland analyser was placed on a triple axis instrument, reflecting part of the beam up at a PSD and the incoming

energy was scanned. 7 parallel $\frac{1}{2}$inch tubes 14 mm apart (far within the possible space of CAMEA) was then cut out of the PSD (and a correction for the different sensitivity at different part of the tube applied).(Se figure 24).

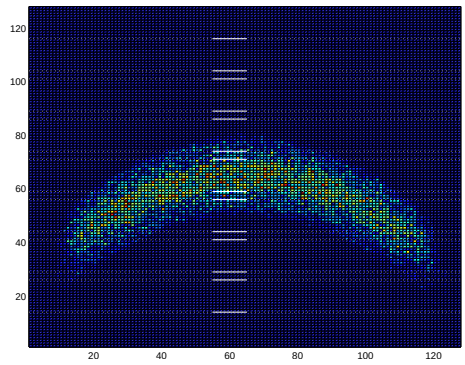

Figure 24: ***Example of psd from simulations.*** *The dotted lines marks the boundaries of the 7 tubes and the solid part the part of the tubes used in the following analysis.*

Figure 25 shows this energy scan for the centre of the tubes for different analyser mosaicities. As it can be seen the tubes sees a well defined Gaussian shaped energy, although each energy overlaps with the one at the neighbour tubes. Unsurprisingly, higher mosaicity means signal in more tubes.

7.2.3 Intensity and Resolution

Figure 26 shows the fitted peak intensity and FWHM from the different tubes and mosaicities. There is no major difference in the width at the different tubes except the expected increase with higher energy. The intensity does of course decrease width the distance from the central tube but for high mosaicities the intensity is quite high in several tubes. Of course one should include the reflectivity of the different analyser crystals in order to get an absolute comparison. So far my simple model suggest that the reflectivity of 90 minutes PG is 0.7 times that of 25 minutes PG if the analysers are 1 mm thick. As a compromise we chose 60' mosaicity and 3 detectors to both increase countrate and improve E and q resolution.

7.2.4 Background

Experience from Rita II shows that a rough collimator in front of the detector, to distinguish different windows, reduce the background a lot. This will be difficult in a set-up where several analysers focus different energies on different detectors. It should, however, not be as important here since all analysers are placed to reflect the same energy at the same q to the detectors. Anyway, in the results above, the tubes are placed 14 mm apart and not the minumum possible 13 mm since this leaves space for a short rough collimation in front of the detectors if necessary.

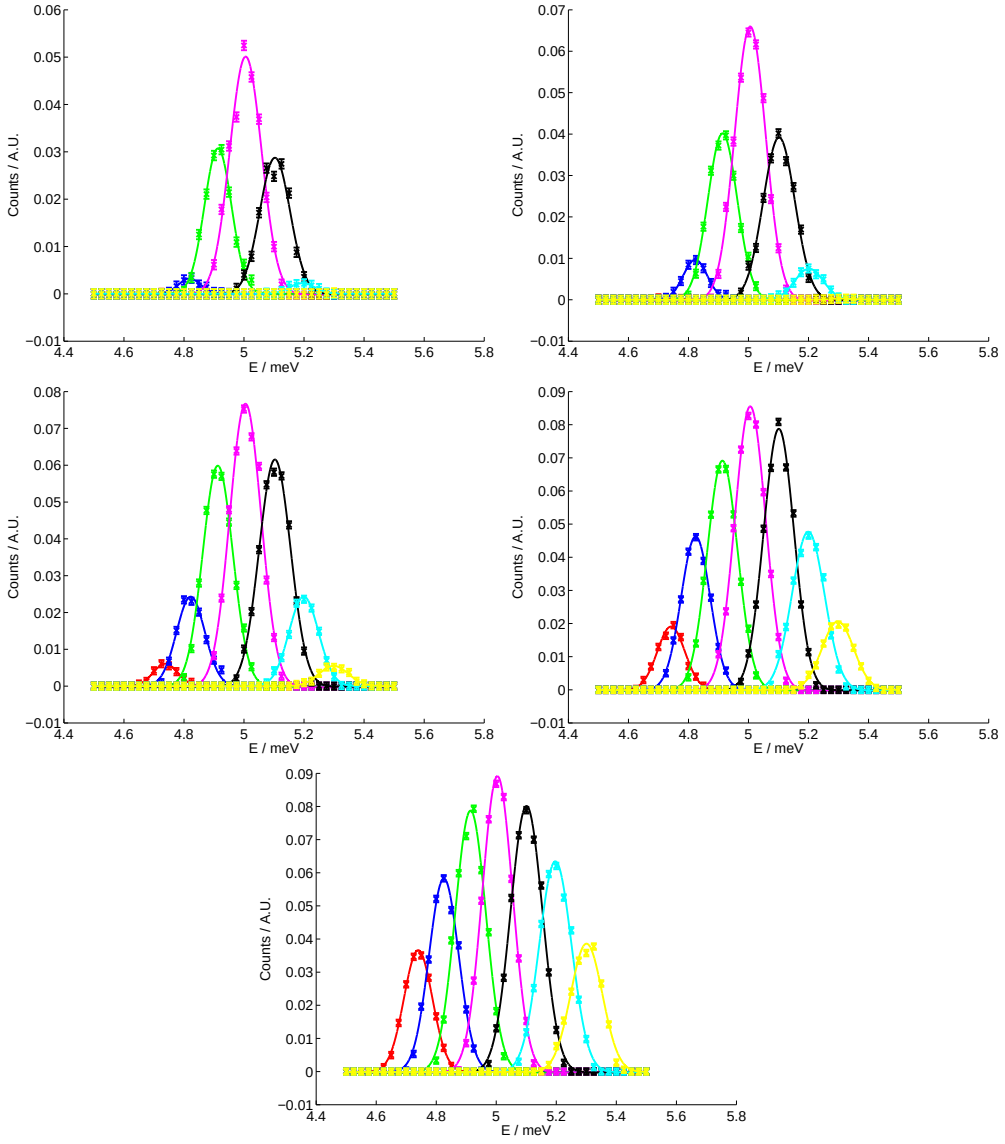

Figure 25: ***Simulated Intensity on detector.*** *The figures shows the simulated intensity in 7 parallel tubes as the incoming energy is scanned for 25, 37, 60, 90, and 120 arch minutes of mosaicity.*

7.2.5 Energy taills

The phonon tails of the strong central reflection as seen on RITA-2 will be relatively stronger compared to the lower flux of the reflections towards the outer tubes. It is thus even more important to reduce the tails in this set-up.

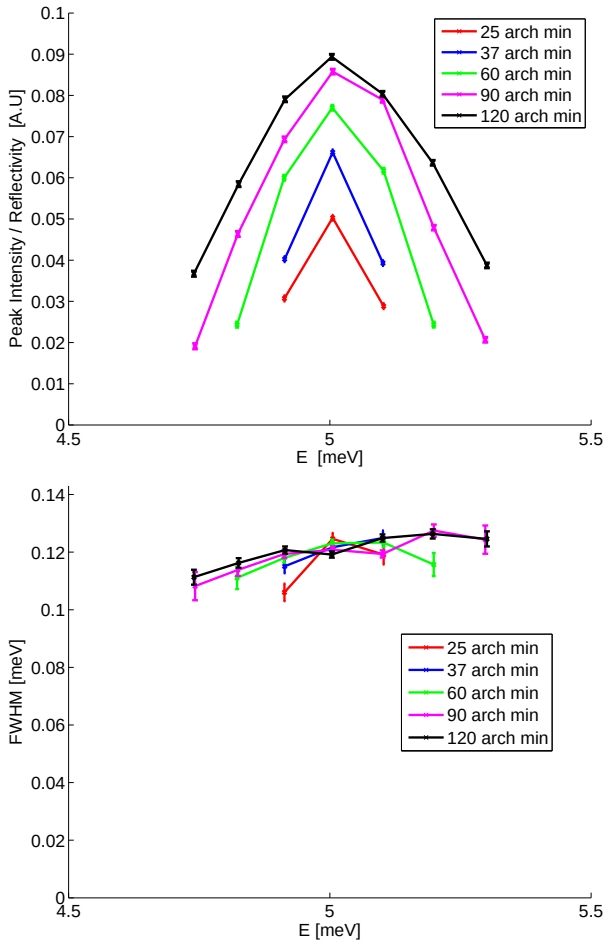

Figure 26: ***Intensity and resolution of the different tubes.*** *The higher the mosaicity the more energies can be measured and the higher the intensity/mosaicity. The FWHM does as expected increase with energy but is almost independent of mosaicity. For both graphs, tubes with sufficiently low statistics were removed since the fitted parameters were to uncertain for any useful conclusions.*

8 Time Resolved measurements

The possibility to do time-resolved neutron scattering on CAMEA was investigated and the time resolution was found to be between 20 μs and 30 μs for most analysers. The main contributions to the resolution is:

8.1 Flightpath uncertainty

The analysers are placed in an asymmetric Rowland Geometry and thus the flight length will vary depending on the neutron scattering position. The effect is bigger the more asymmetric the Rowland geometry. For most analysers an effect of about 10 μs is foreseen whereas the effect for the innermost analysers will be considerably bigger. Both due to more asymmetric setup and lower neutron speed.
For analysers with a high mosaicity and without collimation an uncertainty in the transverse length will also occur but since this is much smaller than the longitudinal travel length it can be neglected.

8.2 Energy uncertainty

The uncertainty in E_f will correspond to an uncertainty in time. If one wants to use time resolution it is therefore advantageous to use the increased energy resolution from the many detectors. If this is used flight time uncertainties become in the order of 10 to 20 μs.

8.3 Uncertainty of scattering position

Since sample has a finite size there is an uncertainty in the exact scattering position. This effect is sample size and energy dependent but in general below 2μ s and thus negligible.

8.4 Uncertainty of detection position

The exact detection position for He^3 tubes is slightly less uncertain than the diameter of the tube as most neutrons are detected in the first part of the detector. On the other hand the round shape of the tubes gives a broadening. Altogether the effect becomes: 3μs.

8.5 Combined Result

Combining the effect and assuming they are independent leads to a total flight time uncertainty of 20-30 μs as described in table 2. Better results can only be obtained by increasing energy resolution and/or decreasing the asymmetry. The uncertainty on the first analysers is mainly due to the asymmetric Rowland Geometry while the uncertainty in at the last analysers mainly arises from energy uncertainty. Generally they are however well matched. The dependency of the energy resolution makes it crucial to use the high resolution mode in time

Analyzer #	1	2	3	4	5	6	7	8	9	10
Energies of analysers (meV)	2.5	2.8	3.1	3.5	4	4.5	5	5.5	6.5	8
Time Resolution (μs)	37	28	23	22	22	22	21	22	21	19

Table 2

resolved studies, but this is anyway foreseen to be the standard operation mode of CAMEA anyway.

9 The Prototype

The main findings in the report were tested against prototype data as the described in the prototype report. The results show a very good agreement between simulations and experiments, strengthening the credibility of the findings. The details are described in the Prototype Report.

10 Conclusion

The use of cheaper coarse mosaic graphite, the possibility to obtain several energies from a single analyser, and the possibility to cover dark angles with sample rotations are direct consequences of simulation results. Together this has led to a cheaper instrument with much better E-resolution and higher coverage but slightly worse q-resolution than originally planned.
Throughout the design process of CAMEA extensive simulations and calculations were performed. The simulations confirms that the instrument will deliver a very high performance, making it possible to investigate a substantial part of the huge parameter space available to the instrument and was key in the design process revealing new possibilities.

[1] ILL Neutron Data Booklet, ed. A.-J. Dianoux and G. Lander, 2003